Technol Rep Yamaguchi Univ 4(5) : 331-344, 1991

Numerical Analysis of Natural Convection Heat Transfer in a Square Enclosure Horizontally or Vertically Divided into Fluid and Porous Regions

Tatsuo NISHIMURA*, Yuji KAWAMURA** and Hiroyuki OZOE***

(Received July 3, 1991)

Abstract

This paper describes an analytical study of laminar natural convection heat transfer in a square enclosure horizontally or vertically divided into fluid and porous regions. The Navier-Stokes equation governs the fluid motion in the fluid region, while Brinkman's extension of Darcy's law is assumed to hold within the porous region. These equations are solved using the Galerkin finite element method in the range $10^3 < Ra_f < 10^5$ and $10^{-3} > Da > 10^{-5}$. The flow patterns are similar for horizontal and vertical divisions. There are two flow modes in the enclosure: circulation over the enclosure and circulation in the fluid region only. Although the flow penetration into the porous region is influenced substantially by the Rayleigh number and the Darcy number, the effect of the Darcy number is more significant. The magnitude of the flow penetration is found to be larger for the vertical division than for the horizontal division.

1. Introduction

The present study is motivated by natural convection during solidification of a binary system. For binary systems, dendritic crystal exists because it is the most efficient morphology for the diffusion of solute and the dissipation of heat in order to reduce the supercooling in the melt.[1] The crystal formation region is referred to as a mushy zone. Figure 1 shows a representative photograph of a mushy zone during solidification of an ammonium chloride-water solution with lateral cooling. Closer examination of the mushy zone reveals a tightly packed array of dendrites of ammonium chloride. Thus fluid flow in the mushy zone has been modelled as natural convection in a porous medium, but penetration of bulk melt into the mushy zone has not been well understood. Penetration of fluid into the mushy zone can significantly alter the local temperatures and concentrations in the mushy zone, eventually leading to macrosegregation.

Hence, as a necessary initial step, the objective of the present study is to investigate the natural convection flow and heat transfer in such a system idealized as a cavity partially filled with a porous medium. Although a similar study has been performed by Beckermann et al.[2,3], there was no available information on the degree of penetra-

*Department of Mechanical Engineering
**Department of Chemical Engineering, Hiroshima University
***Institute of Advanced Material Study, Kyushyu University

tion of bulk liquid into the porous medium. In the present study, we employed a mathematical model different from that developed by Beckermann et al., and solved it using a finite element method.

Although not directly related to the present work, various studies on natural

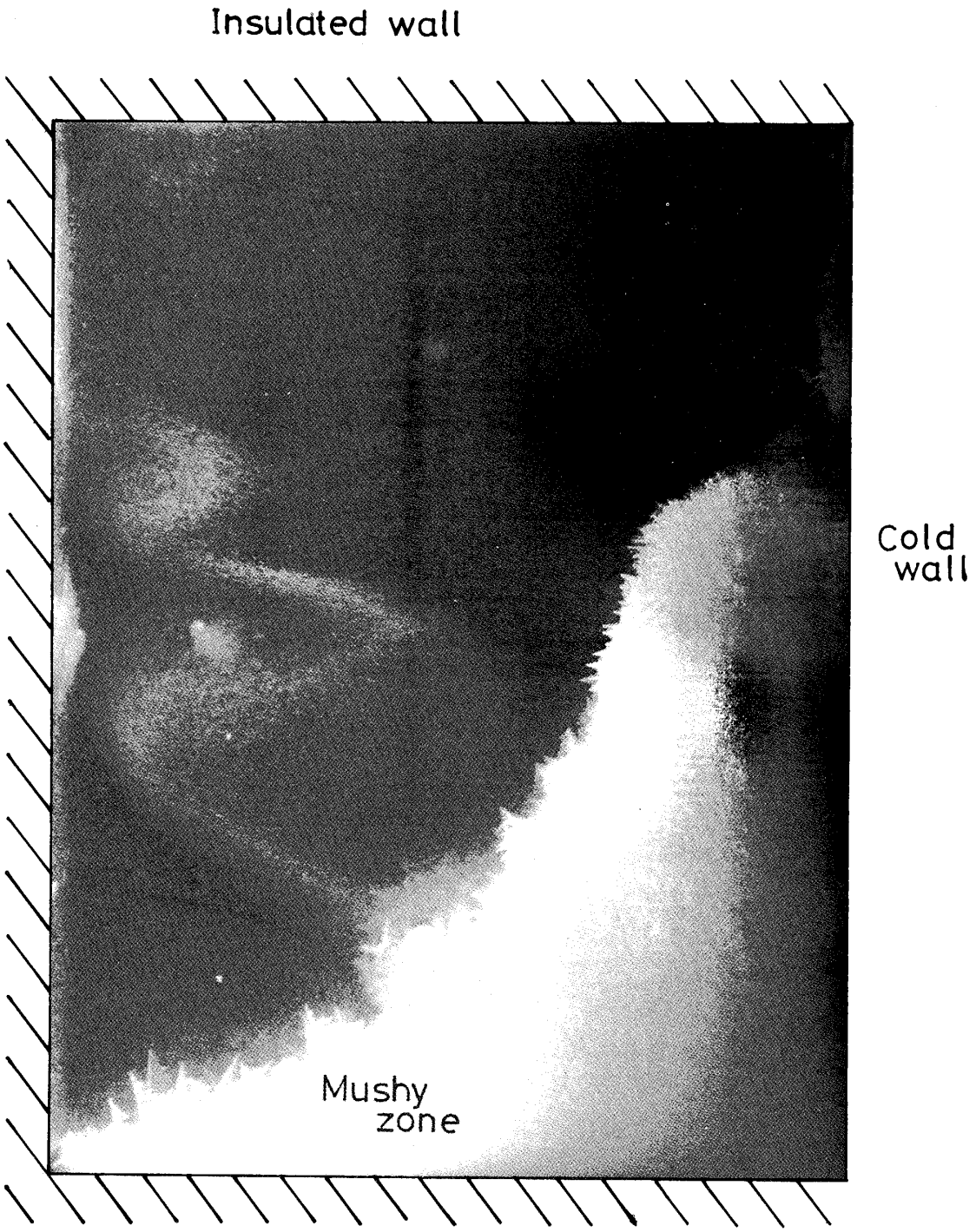

Fig. 1 A mushy zone of ammonium chloride crystal formed by cooling an aqueous solution of ammonium chloride from the side. The photograph is taken by T. Nishimura.

convection in either multiple fluid layers or porous layers have been developed to determine the effect of inhomogeneity on the heat transfer[4-7].

2. Mathematical Model

We consider a two-dimensional square enclosure of length W horizontally or verticlally divided into the fluid and porous regions as shown in Fig. 2. The fluid is assumed to have constant properties, excluding density in a bouyant term, i.e., the Boussinesq approximation is utilized. The porous portion of the enclosure is expressed as W'/W and the interface between fluid and porous regions is straight. The upper and lower walls of the enclosure are insulated, while the vertical walls of the enclosure are isothermal: the right-hand side wall at temperature T_h and the left-hand side at T_c, where $T_h > T_c$.

The Navier-Stokes equation and Darcy's law have been utilized for the fluid motion of the fully-fluid enclosure and for that of the fully-porous enclosure, respectively. However, the combination of the Navier-Stokes equation and Darcy's law leads to discontinuity of velocity, shear stress and pressure at the interface. In order to march the flow conditions at the interface, the Brinkman-extended Darcy equation[8] or the Brinkman-Forchheimer-extended Darcy equation[3] can be used in the porous region. In the two equations, the treatment of inertia term is different. Although Beckermann et al.[2] used the Brinkman-Forchheimer-extended Darcy equation for this system, we used the Brinkman-extended Darcy equation because empritical parameters are not included in this equation.

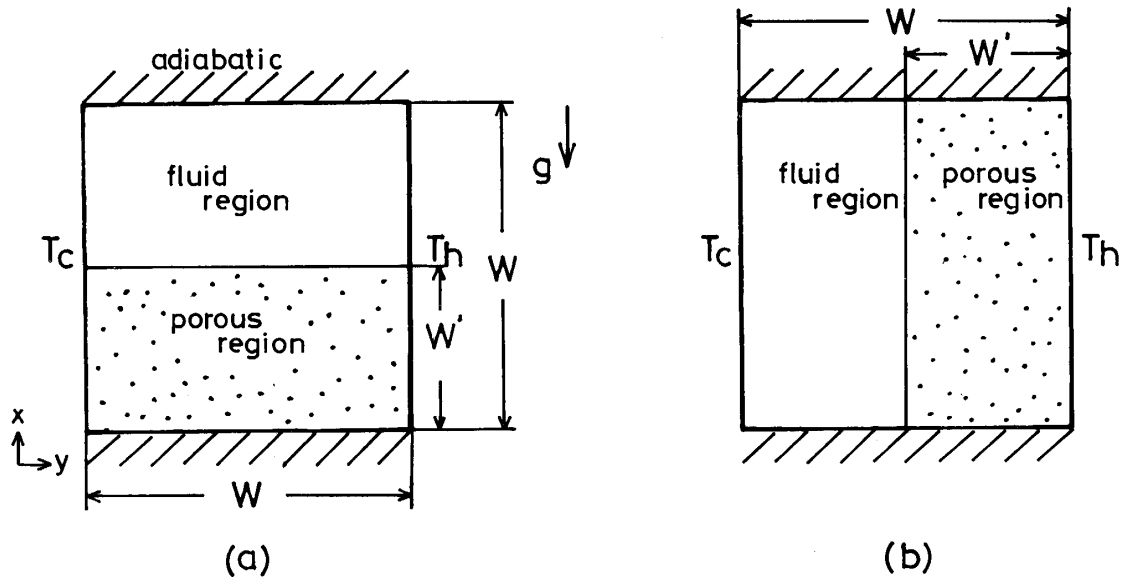

Fig. 2 Schmatic diagram of a square enclosure partially filled with a porous medium.

With the assumptions stated above, the governing equations for this problem are expressed in the following non-dimensional form in terms of stream function, vorticity and termperature:

Fluid region

vorticity transport equation

$$U_f\frac{\partial\xi_f}{\partial X}+V_f\frac{\partial\xi_f}{\partial Y}=Pr_f\nabla^2\xi_f-Ra_fPr_f\frac{\partial\theta_f}{\partial Y} \tag{1}$$

relation between stream function and vorticity

$$\xi_f=-\nabla^2\Psi_f \tag{2}$$

energy transtport equation

$$U_f\frac{\partial\theta_f}{\partial X}+V_f\frac{\partial\theta_f}{\partial Y}=\nabla^2\theta \tag{3}$$

Porous region

vorticity transport equation

$$U_p\frac{\partial\xi_p}{\partial X}+V_p\frac{\partial\xi_p}{\partial Y}=Pr_f\nabla^2\xi_p-(Pr/Da)\,\xi_p-Ra_fPr_f\frac{\partial\xi_p}{\partial Y} \tag{4}$$

relation between stream function and vorticity

$$\xi_p=-\nabla^2\Psi_p \tag{5}$$

energy transport equation

$$U_p\frac{\partial\theta_p}{\partial X}+V_p\frac{\partial\theta_p}{\partial Y}=(\lambda_e/\lambda_f)\nabla^2\theta_p \tag{6}$$

The non-dimensional boundary conditions at four walls of the enclosure and the interface are given as follows:

Horizontal division

$$\text{at } X=0.0 \quad \Psi_p=0.0,\ \xi_p=-\nabla^2\Psi_p,\ \frac{\partial\theta_p}{\partial X}=0.0 \tag{7}$$

$$\text{at } X=1.0 \quad \Psi_f=0.0,\ \xi_f=-\nabla^2\Psi_f,\ \frac{\partial\theta_f}{\partial X}=0.0 \tag{8}$$

$$\text{at } Y=0.0 \quad \Psi_p=0.0,\ \xi_p=-\nabla^2\Psi_p,\ \theta_p=0.0 \text{ for } X<0.5 \tag{9}$$
$$\Psi_f=0.0,\ \xi_f=-\nabla^2\Psi_f,\ \theta_f=0.0 \text{ for } X>0.5$$

$$\text{at } Y=1.0 \quad \Psi_p=0.0,\ \xi_p=-\nabla^2\Psi_p,\ \theta_p=1.0 \text{ for } X<0.5 \tag{10}$$
$$\Psi_f=0.0,\ \xi_f=-\nabla^2\Psi_f,\ \theta_f=1.0 \text{ for } X>0.5$$

at the interface (X=0.5)

$$\Psi_f=\Psi_p,\ \frac{\partial\Psi_f}{\partial X}=\frac{\partial\Psi_p}{\partial X},\ \xi_f=\xi_p,\ \frac{\partial\xi_f}{\partial X}=\frac{\partial\xi_p}{\partial X}-\frac{V_p}{Da} \tag{11}$$

$$\theta_f=\theta_p,\ \lambda_f\frac{\partial\theta_f}{\partial X}=\lambda_e\frac{\partial\theta_p}{\partial X}$$

Vertical division

at X=0.0 $\Psi_f=0.0,\ \xi_f=-\nabla^2\Psi_f,\ \frac{\partial\theta_f}{\partial X}=0.0$ for $Y<0.5$ (12)

$\Psi_p=0.0,\ \xi_p=-\nabla^2\Psi_p,\ \frac{\partial\theta_p}{\partial X}=0.0$ for $Y>0.5$

at X=1.0 $\Psi_f=0.0,\ \xi_f=-\nabla^2\Psi_f,\ \frac{\partial\theta_f}{\partial X}=0.0$ for $Y<0.5$ (13)

$\Psi_p=0.0,\ \xi_p=-\nabla^2\Psi_p,\ \frac{\partial\theta_p}{\partial X}=0.0$ for $Y>0.5$

at Y=0.0 $\Psi_f=0.0,\ \xi_f=-\nabla^2\Psi_f,\ \theta_f=0.0$ (14)

at Y=1.0 $\Psi_p=0.0,\ \xi_p=-\nabla^2\Psi_p,\ \theta_p=1.0$ (15)

at the interface (Y=0.5)

$$\Psi_f=\Psi_p,\ \frac{\partial\Psi_f}{\partial Y}=\frac{\partial\Psi_p}{\partial Y},\ \xi_f=\xi_p,\ \frac{\partial\xi_f}{\partial Y}=\frac{\partial\xi_p}{\partial Y}+\frac{U_p}{Da} \quad (16)$$

$$\theta_f=\theta_p,\ \lambda_f\frac{\partial\theta_f}{\partial Y}=\lambda_e\frac{\partial\theta_p}{\partial Y}$$

Derivation of the equations at the interface is described in the literature[9]. Equations (1) to (6) together with the boundary conditions (Equations (7) to (11)) for the horizontal division and (Equations (12) to (16)) for the vertical division complete the problem definition. These model equations have advantage of being fully predictive, i.e., there is no need for an experimental fit of any parameter.

3. Numerical Calculation

The solution of this problem is dependent on the following parameters: W'/W, λ_e/λ_f, Da, Ra_f and Pr_f. The thermal conductivity ratio, the porous portion of the enclosure and the Parandtl number were held constant ($\lambda_e/\lambda_f=1.0$, W'/W=0.5 and $Pr_f=10$), since the purpose of this study makes clear the difference between the horizontal and vertical divisions in the flow and heat transfer characteristics.

Numerical solutions of Equations (1) to (16) were obtained through use of the Galerkin finite element method. The Solution technique is well described in the literature[10] and has been widely used for natural convection problems involving either pure fluid or porous medium[11,12].

Figure 3 shows a comparison of the present numerical results for a fully fluid enclosure and those previously reported to test the solution technique. The finite element solutions of Nusselt number converge monotonically with increasing the number of mesh. This trend is similar to the result of Ozoe et al.[13]. The Nusselt numbers for a 40×40 mesh agree well with those of other investigations[14-16].

However, for the enclosure divided into fluid and porous regions, the use of this mesh size probably causes a remarkable error in the flow pattern as shown in the previous study[8]. In order to reduce this error, a smaller mesh size in the direction perpendicular to the interface has to be emloyed, in particular near the interface, where a sharp shear stress occurs. For instance, it is necessary to satisfy that the dimensionless mesh size next to the interface, Δh_i is smaller than $\sqrt{Da}$. The reason for this was described in the previous study[8]. Thus we used 0.0005 in Δh_i, which is sufficiently

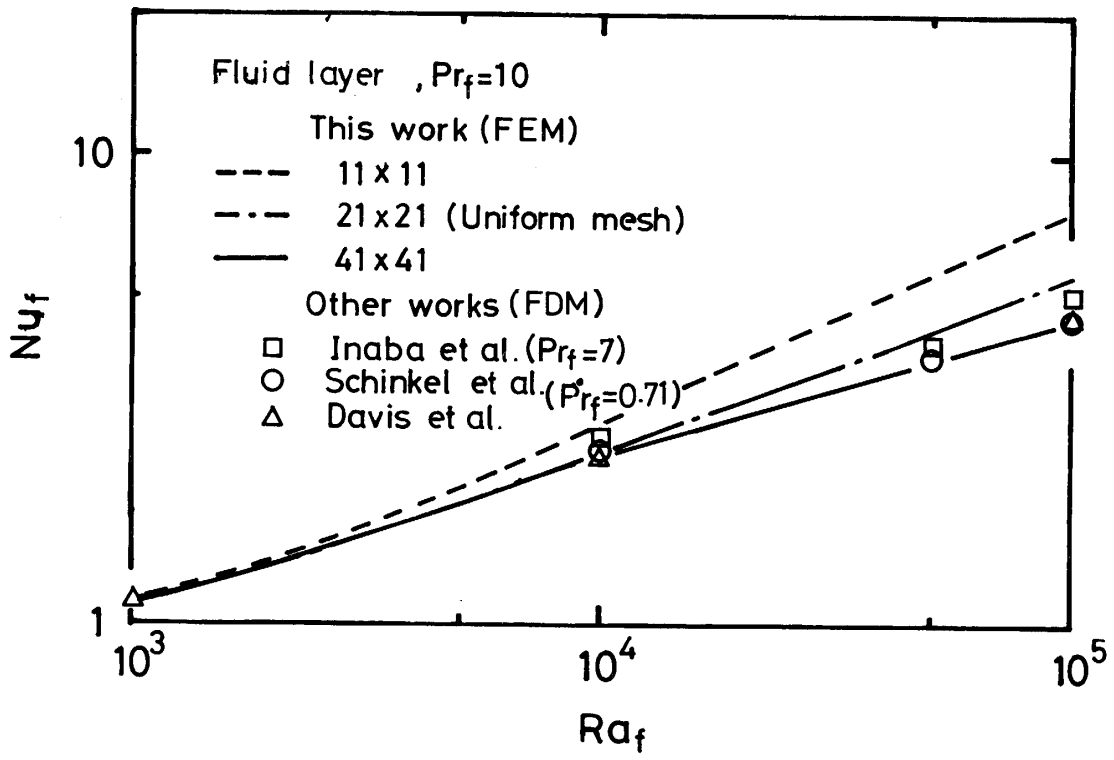

Fig. 3 Comparison of the present calculated Nusselt numbers and those previously reported for a fully-fluid enclosure.

smaller than $\sqrt{Da}$ in the Darcy number range considered here. Figure 4 shows finite element mesh (72×40) for the horizontal division.

4. Computated Results

4.1 *Flow and temperature fields*

Since the flow pattern is the same for Darcy numbers considered here, the streamlines for $Da=10^{-5}$ are presented. Figure 5 shows the result for the horizontal division. The streamline pattern is no longer centrosymmetric as in homogeneous systems; instead, the streamfunction maximum is located in the fluid region. For all Rayleigh numbers, most of the fluid moving downard adjacent to the cold wall in the fluid region goes away from the wall near the interface and then moves along the interface toward the hot wall. While a part of the fluid penetrates into the porous medium. The fluid flowing in the porous region merge with the fluid in the fluid region near the interface at the hot wall. The results are similar to those of a tall enclosure previously reported[8]. For the vertical division, the streamlines have the same pattern as shown in Fig. 6. Thus there are two flow modes for the system consisting of both a fluid region and a fluid-staturated porous region: one is a circulation rotating counter-

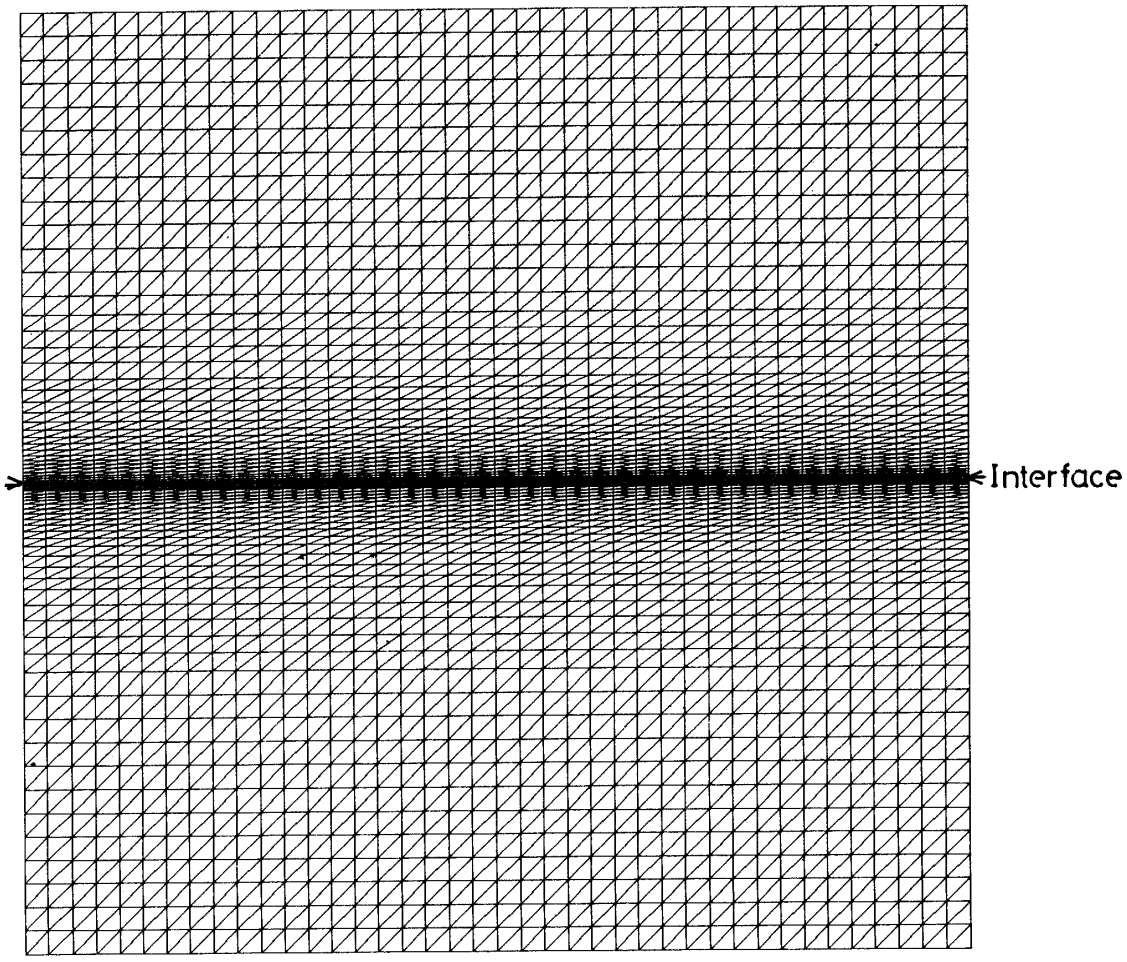

Fig. 4 Finite element mesh for calculation (Horizontal division).

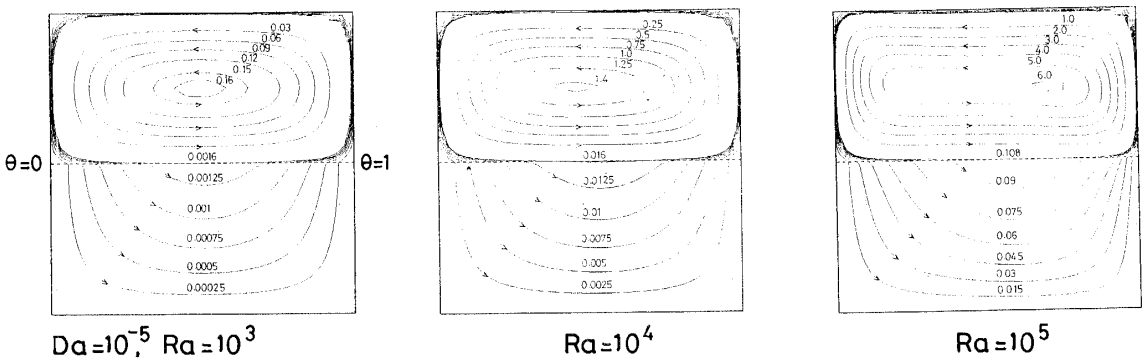

Fig. 5 Variation of streamline patterns with Rayleigh number for $Da=10^{-5}$ (Horizontal division).

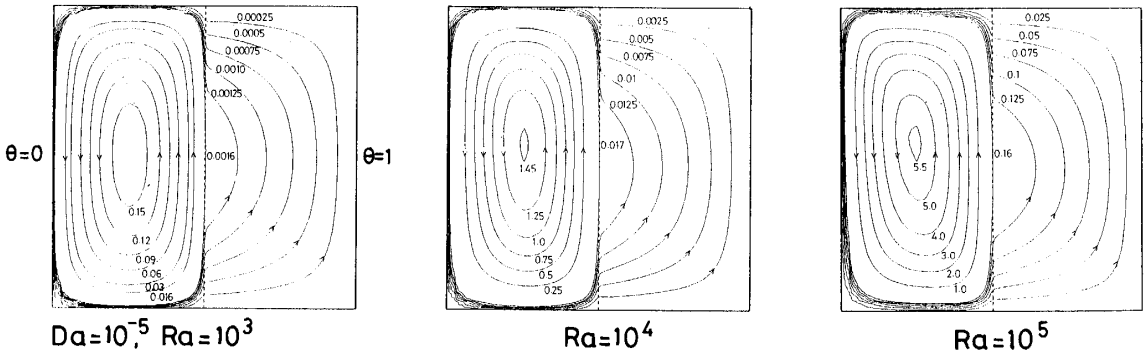

Fig. 6 Variation of streamline patterns with Rayleigh number for $Da=10^{-5}$ (Vertical division).

clockwise in the fluid region only and the other is a circulation with the same rotation over the entire region within the enclosure.

It is interesting to know how the flow penetration from the fluid region into the porous region is varied for the flow parameters of the Darcy number and Rayleigh number. Figure 7 shows the circulation ratio Ψ_w/Ψ_f indicating the degree of flow penetratioin, where Ψ_w is the circulation rate over the entire region and Ψ_f is the circulation rate in the fluid region only, and these are determined by the values of stream function. The solid line and dotted line denote the results of the horizontal and vertical divisions, respectively. In both cases, the circulation ratio gradually increase with the Rayleigh number, and decreases remarkably at a rate which corresponds to a decrease in the Darcy number. The vertical division, however has a larger circulation ratio than the horizontal division, in particular at high Rayleigh numbers. The reason for this is considered that unlike the horizontal division, the fluid does not directly circulates between the hot and cold walls for the vertical division because of the existence of the porous medium covering the hot wall, which leads to an increase of the flow penetration into the porous medium.

Figure 8 shows the variation of isotherms with the Darcy number at $Ra=10^5$ for the horizontal division. The isotherms are similar for any Darcy number in the fluid region, but are quite different in the porous region. This difference is attributed to the flow penetration rate. At $Da=10^{-5}$, the isotherms in the porous region are similar to those for heat conduction only in a solid with no flow, because the flow rate in the porous region is much smaller than that in the fluid region as seen from the value of Ψ_w/Ψ_f shown in Fig. 7. Therefore the isotherms in the fluid region exhibit the same behavior as that for a shallow enclosure (aspect ratio of 0.5) as expected by the streamline pattern shown in Fig. 5. The isotherms for the vertical division are shown in Fig. 9. Since the heat is transferred both fluid and porous regions in series, in contrast to the horizontal division, the isotherms near the hot wall in the porous region become almost straight with decreasing the Darcy number. While the isotherms near

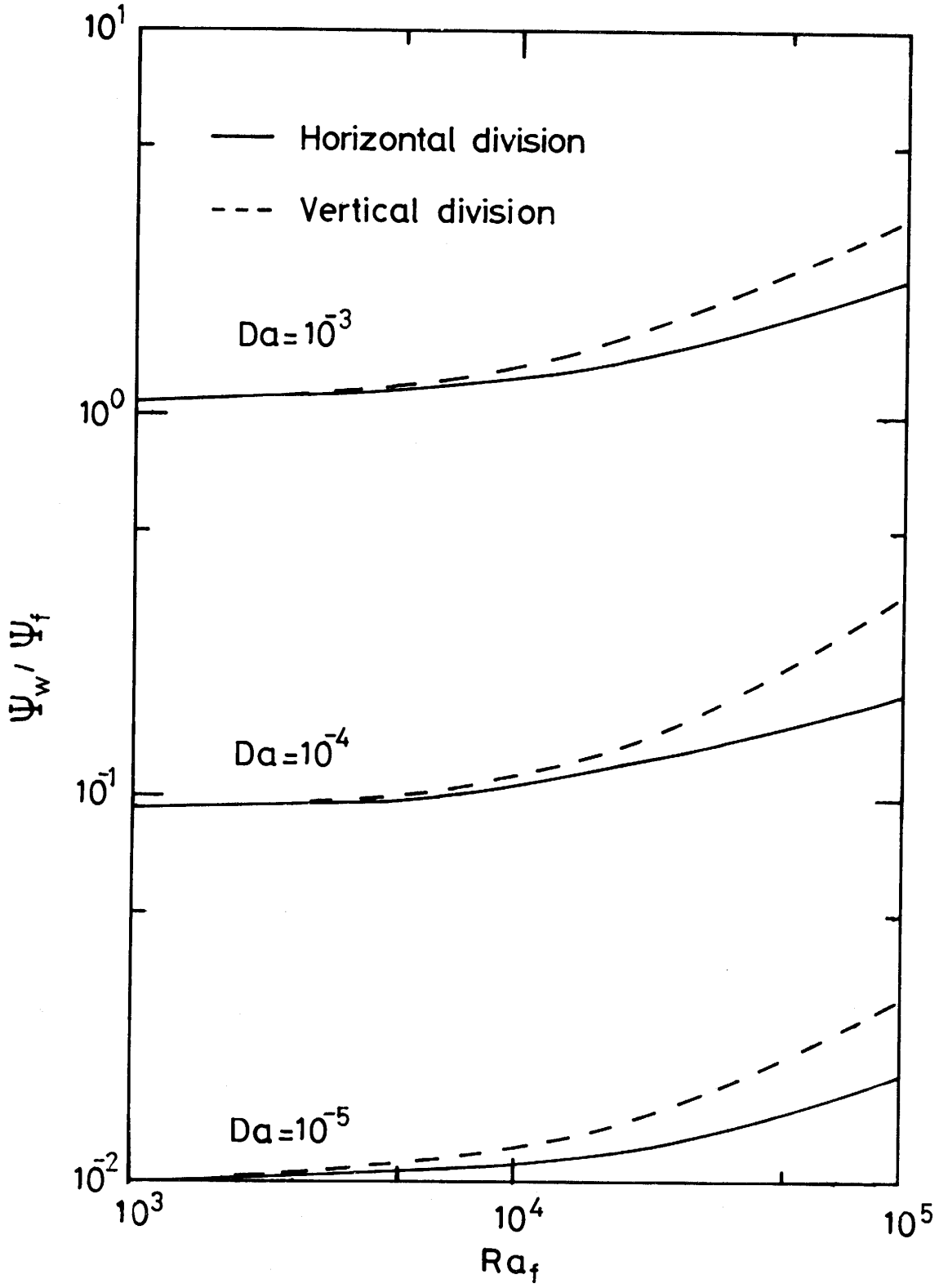

Fig. 7 Variation of flow penetration with Rayleigh number for three different Darcy numbers.

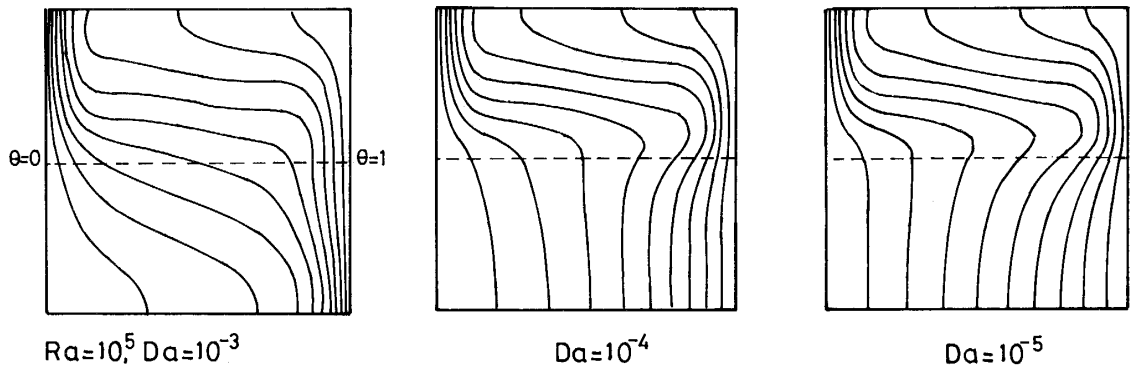

Fig. 8 Variation of isotherms with Darcy number for $Ra=10^5$ (Horizontal division).

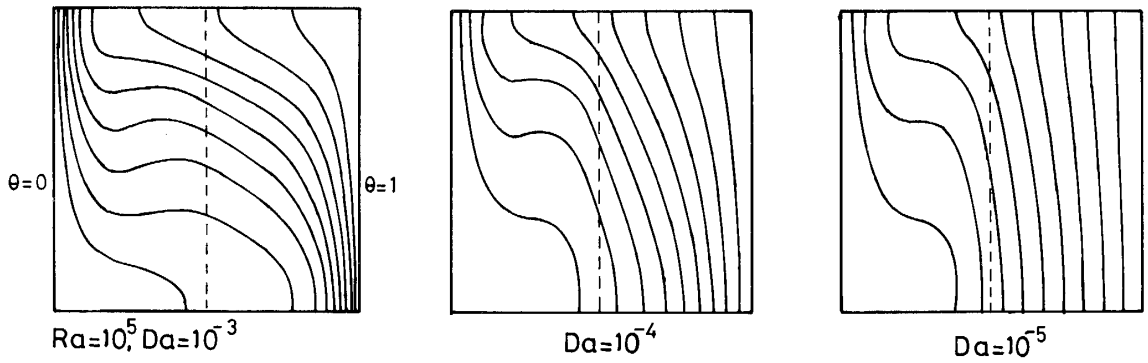

Fig. 9 Variation of isotherms with Darcy number for $Ra=10^5$ (Vertical division).

the cold wall in the fluid region shows a boundary layer structure.

4.2 *Heat transfer rate*

The average Nusselt number is defined as

$$Nu_f = \frac{\text{actual heat transfer rate}}{\text{heat transfer rate by conduction when the entire enclosure is filled with the fluid alone}}$$

and is given in terms of variables of this study as follows (17)

for the horizontal division (at $Y=0$)

$$Nu_f = (\lambda_e/\lambda_f)\int_0^{W'/W}(\partial\theta_p/\partial Y)\,dX + \int_{W'/W}^{1}(\partial\theta_f/\partial Y)\,dX \tag{18}$$

for the vertical division (at $Y=0$)

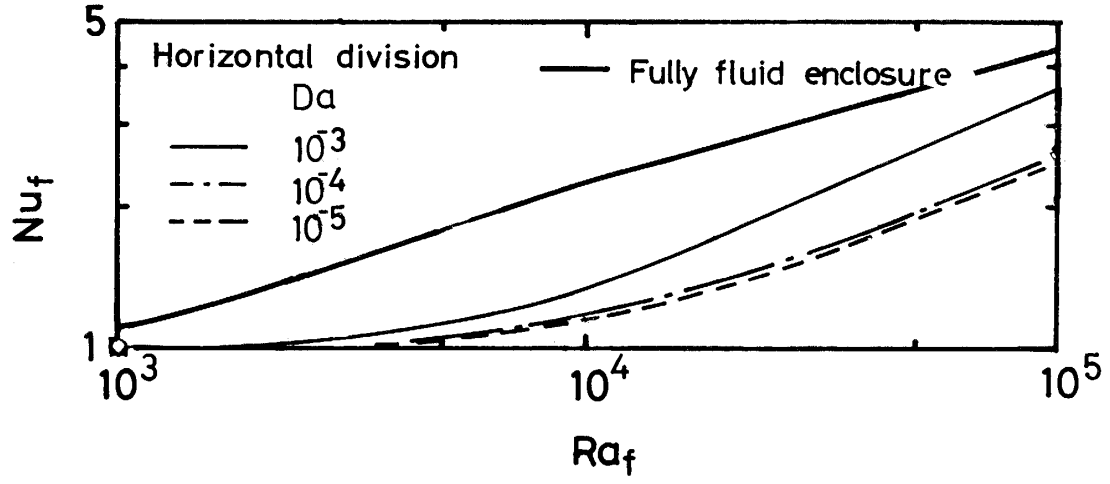

Fig. 10 Variation of Nusselt numbers with Rayleigh number for three different Darcy numbers (Horizontal division).

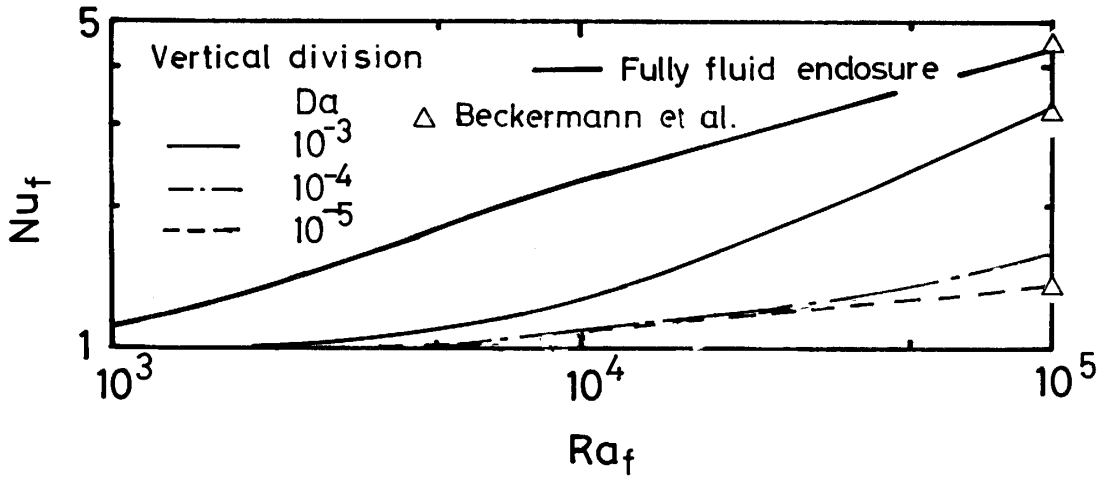

Fig. 11 Variation of Nusselt numbers with Rayleigh number for three different Darcy numbers (Vertical division).

$$Nu_f = \int_0^1 (\partial\theta_f/\partial Y)\,dX \tag{19}$$

where the temperature gradient is evaluated at the cold wall $Y=0$.

Figure 10 shows the relationship between the Nusselt number and the Rayleigh number for the horizontal division. The Nusselt number for any Darcy number is smaller than that for the fully-fluid enclosure, and decreases with the Darcy number at large Rayleigh numbers, but makes little difference for $Da=10^{-4}$ and 10^{-5}. This result deduces that the flow in the porous region hardly affect the heat transfer rate.

The vertical division is shown in Fig. 11. The present results agree well with those of Beckermann et al.[2], even for a large Darcy number, i.e., $Da=10^{-3}$, although the mathematical models are different in the inertia term of the governing equation in the porous region as mentioned in section 2. The Nusselt number for the vertical division has a smaller value than that for the horizontal division. This is because the heat is transferred in series and parallel through the fluid and porous regions for the vertical and horizontal divisions, respectively. In particular the trend becomes more significant with decreasing the Darcy number. This is also expected from the behavior of isotherms near the hot wall in Figs. 8 and 9.

5. Conclusions

Natural convection heat transfer in a square enclosure horizontally or vertically divided into fluid and porous regions was analyzed numerically. The Navier-Stokes equation and Brinkman's equation were used for the fluid motion in the fluid region and for that in the porous region, respectively. These equations were solved by the Galerkin finite element method.

The flow patterns are similar for the horizontal and vertical divisions. There are two flow modes in the enclosure: circulation over the enclosure and circulation in the fluid region only. However, the intensity of circulation is always much stronger in the fluid region than in the porous region. The magnitude of penetration of flow from the fluid region into the porous region is influenced substantially by the Rayleigh number and the Darcy number. The vertical division has a larger penetration than the horizontal division as the Rayleigh number increases.

Although the present analysis is limited to heat transfer, heat and mass transfer which is important for solidification of a binary system will be analyzed by extension of the numerical procedure in the future.

Nomenclature

Da	Darcy number, κ/W^2
g	gravitational acceleration
Nu_f	Nusselt number
Pr_f	Prandtl number of the fluid
Ra_f	Rayleigh number, $g\beta(T_h-T_c)W^3/\alpha_f\nu_f$
T	temperature
T_c	temperature at the cold wall
T_h	temperature at the hot wall
U	dimensionless vertical velocity, uW/α_f
u	vertical velocity
V	dimensionless horizontal velocity, vW/α_f
v	horizontal velocity
W	width of the enclosure
X	dimensionless vertical coordinate, x/W
x	vertical coordinate

Y	dimensionless horizontal coordinate, y/W
y	horizontal coordinate
α_e	thermal diffusivity of the porous medium
α_f	thermal diffusivity of the fluid
β	volumetric expansion coefficient
θ	dimensionless temperature, $(T-T_c)/(T_h-T_c)$
κ	permeability
λ_e	effective thermal conductivity of the porous medium
λ_f	thermal conductivity of the fluid
ν_f	kinematic viscosity of the fluid
Ψ	dimensionless stream function, ψ/α_f
Ψ_f	circulation in the fluid region only
Ψ_w	circulation over the entire region
ψ	streamfunction
Ω	dimensionless vorticity, $\omega W^2/\alpha_f$
ω	vorticity
Δh_I	dimensionless mesh size in the porous region next to the interface

Subscripts

f	fluid region
p	porous region

References

1) Ohno, A. "An Introduction to the Solidification of Metals", Chijin Shyokan, p.26-28(1990) (in Japanese).
2) Beckermann, C., Ramahyani, S. and Viskanta, R. "Natural Convection Flow and Heat Transfer Between Fluid Layer and a Porous Layer Inside a Rectanglular Enclosure" J. Heat Transfer, **109**, 363-370(1987).
3) Beckermann, C., Viskanta, R. and Ramahyani, S. "Natural Convection in Vertical Enclosure Containing Simultaneously Fluid and Porous Layers" J. Fluid Mech., **186**, 257-284(1988).
4) Sparrow, E.M., Azevedo, L.F.A. and Prata, A.T. "Two-Fluid and Single-Fluid Natural Convection Heat Transfer in a Enclosures" J. Heat Transfer, **108**, 848-852(1986).
5) Poulikakos, D. and Bejan, A. "Natural Convection in Vertically and Horizontally Layered porous Media Heated from the Side" Int. J. Heat Mass Transfer, **26**, 1805-1814(1983).
6) Masuoka, T., Narazaki, K., Tsuruta, T. and Tohda, Y. "Natural Convection in Stratified Porous Media Heated from the Side" Trans JSME Ser.B, **52**, 866-869(1986) (in Japanese).
7) Szekely, J. and Todd, M.R. "Natural Convection in a Rectangular Cavity Transient Behavior and Two Phase Systems in Laminar Flow" Int. J. Heat Mass Transfer, **14**, 467-482(1971).
8) Nishimura, T., Takumi, T., Shiraishi, M., Kawamura, Y. and Ozoe, H. "Numerical Analysis of natural Convection in a Rectangular Enclosure Horizontally Divided into Fluid and Porous Regions", Int. J. Heat Mass Transfer, **29**, 889-898(1986).
9) Nandakumar, K. and Masliyah, J.H. "Laminar Flow past a Permeable Sphere" Can. J. Chem. Engng., **60**, 202-211(1982).
10) Tabarrok, B. and Lin, R.C. "Finite Element Analysis of Free Convection Flows" Int. J. Heat Mass Transfer, **20**, 945-952(1977).
11) Nishimura, T., Kawamura, Y., Takumi, T. and Ozoe H. "Analysis of Natural Convection Heat Transfer at the Walls of Packed Beds with Voidage Variations" Heat Transfer Japanese Research, **14**, 47-54(1985).

12) Nishimura, T., Shiraishi, M. and Kawamura, Y. "Analysis of Natural Convection Heat Transfer in Enclosures Divided by a Vertical Partition Plate" Heat Transfer Science and Technology, pp. 129-136. Hemisphere, Washington, DC, (1987).
13) Ozoe, H. Hatano, T., Sayama, H. and Churchill, S.W. "Use of the Finite Element Method for Natural Convection in a Horizontally Confined Infinite Layer Fluid" Numer. Heat Transfer, **6**, 55-66 (1983).
14) De Vahl Davies, D. and Jones, I.P. "Natural Convection in a Square Cavity: A Comparison Exercise", AERE-P9955, Harwell, Oxfordshire, U.K. (1981).
15) Inaba, H., Seki, N. and Fukusako, S. "Heat Transfer by Natural Convection in a Shallow Rectangular Cavity with Two Opposing Vertical Walls at Different Temperatures", Bulletin of the JSME, **25**, 939-943 (1982).
16) Schinkel, W.M.M., Linthorst, S.J.M. and Hoogendorn, C.J. "The Straitification in Natural Convection in Vertical Enclosures" J. Heat Transfer, **105**, 267-272 (1983).